Harmonic and Interharmonic Frequency Estimation for Power Systems via Segmented Coprime Sampling

YUE Heng[1,2], *ZHANG Xiaofei*[1,2*]

1. Key Laboratory of Dynamic Cognitive System of Electromagnetic Spectrum Space, Nanjing University of Aeronautics and Astronautics, Nanjing 211106, P. R. China;

2. College of Electronic and Information Engineering, Nanjing University of Aeronautics and Astronautics, Nanjing 211106, P. R. China

Abstract: The number of harmonics generated by power electronics in power systems is increasing, and the harmonic problem is a significant concern. In this paper, we propose an improved coprime sampling (CS) scheme for harmonic and interharmonic frequency estimation. The proposed scheme uses sparse sampling to reduce the sampling rate significantly and combines it with modern spectral estimation algorithms. Then, the segmented coprime sampling (SCS) method replaces the traditional CS, effectively reducing the sampling rate and the hardware system's workload. In addition, the root-multiple signal classification (root-MUSIC) algorithm returns the commonly used MUSIC algorithm, which guarantees estimation accuracy and significantly reduces computational complexity. The simulation results show that the proposed scheme outperforms the traditional uniform sampling (US) method in estimation accuracy.

Key words: coprime sampling; interharmonic; root-multiple signal classification (MUSIC) algorithm; frequency estimation

CLC number: TN911   **Document code:** A   **Article ID:** 1005-1120(2023)01-0071-09

0 Introduction

As energy technologies have been developed rapidly in recent years, increasing power electronics have been added to the power grid, which leads to intermittent harmonics with variable frequencies. Thus, a variety of problems arise, such as pollution of electrical energy, increased energy losses, reduced power system reliability, and new monitoring challenges[1-2]. Therefore, harmonic and interharmonic analysis is significant for monitoring and protecting power systems[3].

Harmonic and interharmonic detection systems utilize the Nyquist sampling theorem[4-6]. As the harmonic and interharmonic detection process becomes increasingly complex[7-8], the signal is usually sampled for tens of fundamental frequency cycles, and the detection is poor in real-time[9]. Effective harmonic estimation methods have become a hot topic. Until now, many new methods have been proposed, and different researchers have conducted studies. Refs.[10-11] proposed a sub-Nyquist sampling technique and improved it to reduce the sampling burden. Ref.[12] proposed an interpolation fast Fourier transform (FFT) algorithm based on the Hanning window, and Ref.[13] used the multiple signal classification (MUSIC) algorithm to estimate harmonics and interharmonics.

Modern spectrum estimation methods have been widely used for fault diagnosis, aerospace, and direction of arrival (DOA) estimation[14-16] due to their higher frequency resolution, adaptability, and more accurate frequency detection of sinusoidal

signals, which can be used to overcome the drawbacks present in discrete Fourier transform (DFT) algorithms.

For the DOA estimation problem of sparse arrays, many improved techniques have been proposed to improve the estimation accuracy and reduce the amount of computation. The proposed coprime array[17], nested array[18], and minimal redundancy array[19] all have large array apertures. Among these arrays, the nested array is composed of two parts: Continuous array elements and sparse array elements with large intervals. If the nested array is used as a sampling configuration, it will lead to a relatively high sampling rate and increase the hardware burden. The minimal redundancy array is used as a sampling configuration to avoid sampling at the Nyquist rate, but there is no closed-form expression for the sampler. The coprime array is used as a sampling configuration that can fully achieve sparse sampling, and there are various extensions available to improve the array aperture.

Compared with traditional coprime sampling methods, the recently proposed segmented coprime sampling (SCS) schemes have received increasing attention in frequency estimation[20]. Ref.[20] adopted the SCS scheme to estimate the frequency of the weak linear frequency modulated signals, which reduced the sampling rate, and the estimation performance was also close to the traditional method.

In this paper, inspired by the sparse array DOA estimation techniques[21-22], we propose a harmonic and interharmonic frequency estimation scheme based on segmented coprime sampling. First, the proposed scheme uses sparse sampling to obtain sparsely sampled received data. Second, in order to obtain high-resolution estimation results, the sample data are analyzed by the root-MUSIC algorithm. The proposed scheme is applicable to harmonic and interharmonic signals in power systems, and the sparse sampling process reduces the sampling burden, while modern spectral estimation algorithms can obtain accurate frequency estimates. In summary, this paper makes the following contributions.

(1) We construct the received data of the harmonic and interharmonic signals of the power system, applicable to frequency estimation under coprime sampling.

(2) We improve the sampling process of coprime sampling[23], and effectively reduce the sampling rate by alternating the two sets of samplers.

(3) We propose a frequency estimation scheme based on segmented coprime sampling, apply modern spectrum estimation methods to the harmonic estimation problem of power systems, and use the root-MUSIC algorithm instead of the MUSIC algorithm to reduce the computational complexity of the overall scheme.

1 Data Model

1.1 Signal model

The power system frequency signal containing noise, harmonic, and interharmonic is expressed as follows[24]

$$f(t)=\sum_{d=1}^{D}\alpha_d\sin(\omega_d t+\varphi_d)+e(t) \qquad (1)$$

where D is the number of sinusoidal components, including fundamental, harmonic and interharmonic; α_d the amplitude of the dth sinusoidal component; ω_d the angular frequency of the dth sinusoidal component; φ_d the phase of the dth sine wave component, which is uniformly distributed in $(-\pi,\pi)$ statistically independent; and $e(t)$ the noise signal. Eq.(1) can be transformed into Eq.(2)[9].

$$x(t)=\sum_{d=1}^{D}\alpha_d e^{j(\omega_d t+\varphi_d)}+u \qquad (2)$$

where u is the uncorrelated complex Gaussian white noise with zero mean.

1.2 Segment coprime sampling

Fig.1 illustrates the sampler for coprime sampling and segmented coprime sampling, both of which contain two sets of sub-Nyquist samples. The difference is that the two sets of samples for segmented coprime sampling are alternated instead of being
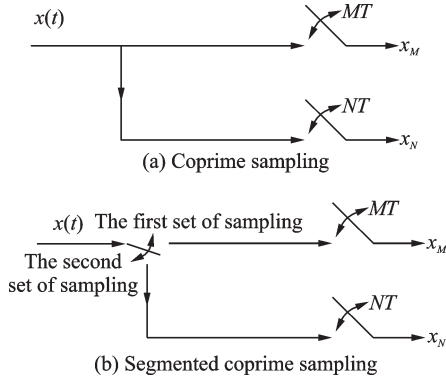
Fig.1   Coprime sampling and segmented coprime sampling

performed simultaneously, where M and N are coprime integers, and T represents the Nyquist sam-

pling interval.

According to Ref.[25], two sets of samplers are used to sample the signal to be measured with sampling time spacing and, where represents the Nyquist sampling frequency. The following example shows the sampled signals in the l ($l \geqslant 0$) units of both sets of samplers.

Fig.2 illustrates segmented coprime sampling with two sets of samplers, along with the sampling time for the two sets. Two sets of samplers are sampled alternately once to get the sample data of one unit, as shown in Eqs.(3,4).
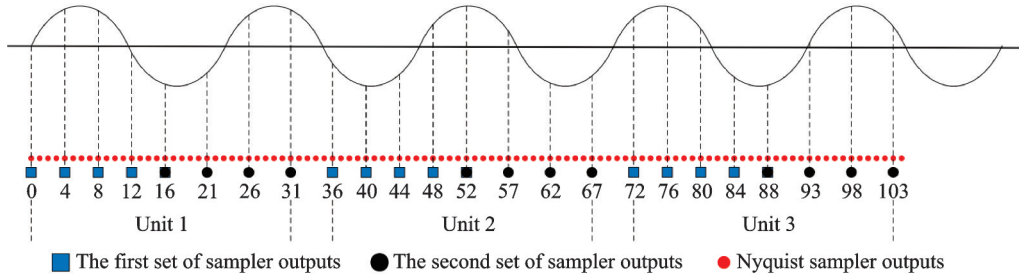

Fig.2   Sampling time for the two sets ($M=4$ and $N=5$)

$$x_M[(M+N-1)l+n]=$$
$$\sum_{d=1}^{D}\alpha_d \mathrm{e}^{\mathrm{j}((2MN-M-N)l+Mn)\omega_d T+\varphi_d)} +$$
$$u((2MN-M-N)l+Mn)T) \qquad (3)$$
$$x_N[(M+N-1)l+N+m]=$$
$$\sum_{d=1}^{D}\alpha_d \mathrm{e}^{\mathrm{j}(((2MN-M-N)l+(N-1)M+mN)\omega_d T+\varphi_d)} +$$
$$u((2MN-M-N)l+(N-1)M+mN)T) \qquad (4)$$

where $m(1\leqslant m\leqslant M-1)$ and $n(0\leqslant n\leqslant N-1)$ are the number of samples in each group of samplers.

As explained above, we can use two subsets of samples to compose a sampled signal vector, shown as

$$y_M(l)=[x_M((M+N-1)l+0),$$
$$x_M((M+N-1)l+1),\cdots,$$
$$x_M((M+N-1)l+N-1)]^{\mathrm{T}} \qquad (5)$$
$$y_N(l)=[x_N((M+N-1)l+N+1),$$
$$x_N((M+N-1)l+N+2),\cdots,$$
$$x_N((M+N-1)l+N+M-1)]^{\mathrm{T}} \qquad (6)$$

Concatenating the samples of the two subsets,

the signal vector of the entire sampled signal can be expressed as follows

$$y(l)=\begin{bmatrix} y_M(l) \\ y_N(l) \end{bmatrix}=$$
$$\sum_{d=1}^{D}a(\omega_d)\alpha_d \mathrm{e}^{\mathrm{j}\varphi_d}\mathrm{e}^{\mathrm{j}(2MN-M-N)l}+u=$$
$$As(l)+u \qquad (7)$$

where $A=[a(\omega_1),a(\omega_2),\cdots,a(\omega_D)]$ is the frequency matrix, here $a(\omega_d)$ is a frequency vector containing a single frequency information, which is denoted as

$$a(\omega_d)=[1,\mathrm{e}^{\mathrm{j}M\omega_d T},\cdots,\mathrm{e}^{\mathrm{j}(N-1)M\omega_d T},$$
$$\mathrm{e}^{\mathrm{j}((N-1)M+N)\omega_d T)},\cdots,\mathrm{e}^{\mathrm{j}((N-1)M+(M-1)N)\omega_d T}]^{\mathrm{T}}$$

and $s(l)$ is denoted as

$$s(l)=[A_1 \mathrm{e}^{\mathrm{j}((2MN-M-N)l\omega_1 T+\varphi_1)},$$
$$A_2 \mathrm{e}^{\mathrm{j}((2MN-M-N)l\omega_2 T+\varphi_2)},\cdots,$$
$$A_D \mathrm{e}^{\mathrm{j}((2MN-M-N)l\omega_D T+\varphi_D)}]^{\mathrm{T}}$$

2   Frequency Estimation

According to Ref.[26], the segment coprime sampling using MUSIC methods for directly estimating parameters does not produce any ambigui-

ties. Root-MUSIC is a polynomial rooting version of the MUSIC algorithm, whose main idea is the Pisarenko decomposition. It consists of the following steps.

(1) Calculate the corresponding covariance matrix, that is

$$\hat{R}_Y = E\left[y(l) y^H(l) \right] =$$
$$\sum_{d=1}^{D} \alpha_d^2 a(\omega_d) a^H(\omega_d) + \sigma_n^2 I =$$
$$A R_S A^H + \sigma_n^2 I \tag{8}$$

where $R_S = \mathrm{diag}\left[p_1, p_2, \cdots, p_D \right]$, $p_d = \alpha_d^2$, I is an identity matrix, σ_n^2 the noise power, $\mathrm{rank}(\hat{R}_Y) = S$, $\mathrm{rank}(R_S) = D$, and $\mathrm{rank}(\cdot)$ represents the rank of the matrix.

According to Eq.(8), the noise subspace can be obtained by performing eigen-decomposition on the obtained covariance matrix, that is

$$\hat{R}_Y = E_s \Lambda_s E_s^H + E_n \Lambda_n E_n^H \tag{9}$$

where Λ_s denotes a $D \times D$ dimensional diagonal matrix whose diagonal elements contain the larger D eigenvalues obtained from the eigenvalue decomposition, Λ_n a diagonal matrix consisting of $S-D$ smaller eigenvalues, E_s the signal subspace, and E_n the noise subspace.

(2) Define the polynomial and solve

$$p_k(z) = u_k^H p(z) \quad k = D+1, \cdots, M+N-1 \tag{10}$$

where u_k is the kth eigenvector of the covariance matrix $\hat{R}_Y$, z the surrogate parameter, and $p(z) = \left[1, z^M, \cdots, z^{(N-1)M}, \cdots, z^{(N-1)M+(M-1)N} \right]$.

In order to extract information from all eigenvectors simultaneously, it is necessary to find the zeros for the denominator $p^H(z) \Lambda_n \Lambda_n^H p(z)$ of the MUSIC spectral function. Since only the value of z on the unit circle is required, $p^T(z^{-1})$ should be substituted for $p^H(z)$.

Substituting a polynomial in z for the above polynomial, we obtain

$$F(z) = z^{[(N-1)M+(M-1)N]} p^T(z^{-1}) \Lambda_n \Lambda_n^H p(z) \tag{11}$$

As $z = e^{j\omega_d}$, p belongs to the signal subspace, $F(z) = 0$, which is the polynomial on the unit circle of the roots corresponding to the sinusoidal signal's frequency. The D roots of polynomial $F(z)$ closest

to the unit circle $z_1, z_2, \cdots, z_D$ are found, corresponding conjugate roots for $(z_1^*, z_2^*, \cdots, z_D^*)$.

(3) Estimate harmonic and interharmonic frequencies calculated from the follow of polynomial. Thus, the frequency of the complex sine signal can be calculated as follows

$$f_d = \frac{\arg(z_d)}{2\pi T} = \frac{\omega_d}{2\pi T} \quad d = 1, 2, \cdots, D \tag{12}$$

where arg ($\cdot$) is the operation of phase angle.

Finally, we obtain harmonic and interharmonic frequency estimation schemes for segmented coprime sampling, and the main process can be summarized as follows.

Algorithm 1 Frequency estimation via segmented coprime sampling

Input: The sampled signal vector y (l) in Eq.(7) and the number of frequencies D

Covariance matrix:

(1) According to Eq.(8), calculate the covariance matrix of the sampled signal $\hat{R}_Y$;

(2) According to Eq.(9), perform eigenvalue decomposition on the covariance matrix, select the largest first D eigenvalues to construct the signal subspace, and use the remaining eigenvalues to construct the noise subspace.

Root-MUSIC:

(1) Define Eq.(10);

(2) Substitute a polynomial in z for Eq.(11);

(3) Find the D roots of polynomial $F(z)$ closest to the unit circle $z_1, z_2, \cdots, z_d$;

(4) According to Eq.(12), use the z obtained by solving the polynomial to obtain the estimated value of the frequency f_d.

Output: Estimated value of the frequency f_d.

3   Performance Analysis

3.1   Cramér Rao bound

The purpose of this section is to provide the Cramér Rao bound (CRB) for segment coprime sampling. According to Ref.[25], the parameter vectors of the signal model (Eq.(7)) are defined as follows

$$r = \text{vec}(\hat{\boldsymbol{R}}_Y) =$$

$$\sum_{d=1}^{D} \alpha_d^2 \boldsymbol{a}^*(\omega_d) \otimes \boldsymbol{a}(\omega_d) + \sigma_n^2 \boldsymbol{i} =$$

$$\boldsymbol{A}_c \boldsymbol{p} + \sigma_n^2 \boldsymbol{i} \qquad (13)$$

where $\otimes$ denotes the Kronecker product, $\boldsymbol{A}_c = \boldsymbol{A}^* \odot \boldsymbol{A}$, $\boldsymbol{p} = [p_1, p_2, \cdots, p_D]^T$, $\boldsymbol{i} = \text{vec}(\boldsymbol{I})$, here $\text{vec}(\bullet)$ is the operation of vectorization and $\odot$ denotes the Khatri-Rao product.

$$\boldsymbol{\eta} = [\omega_1, \cdots, \omega_D, p_1, \cdots, p_D, \sigma_n^2]^T \qquad (14)$$

The (i, j)th element of the fisher information matrix ($\boldsymbol{FIM}$) can be shown as follows

$$\text{FIM}_{i,j} = L \, \text{trace}\left[\frac{\partial \hat{\boldsymbol{R}}_Y}{\partial \eta_i} \hat{\boldsymbol{R}}_Y^{-1} \frac{\partial \hat{\boldsymbol{R}}_Y}{\partial \eta_j} \hat{\boldsymbol{R}}_Y^{-1}\right] \qquad (15)$$

where $\text{trace}(\bullet)$ refers to the trace of the matrix.

Based on a similar derivation in Ref.[27], FIM can be given as follows

$$\text{FIM} = L \begin{bmatrix} \boldsymbol{M}_f^H \boldsymbol{M}_f & \boldsymbol{M}_f^H \boldsymbol{M}_s \\ \boldsymbol{M}_S^H \boldsymbol{M}_f & \boldsymbol{M}_S^H \boldsymbol{M}_S \end{bmatrix} \qquad (16)$$

where $\boldsymbol{M}_f = (\hat{\boldsymbol{R}}_Y^T \otimes \hat{\boldsymbol{R}}_Y)^{-\frac{1}{2}} \boldsymbol{A}_d \boldsymbol{R}_s$, $\boldsymbol{M}_s = (\hat{\boldsymbol{R}}_Y^T \otimes \hat{\boldsymbol{R}}_Y^T)^{-\frac{1}{2}} [\boldsymbol{A}_c, \boldsymbol{i}]$ and $\boldsymbol{A}_d = \boldsymbol{A}_{\text{der}}^* \odot \boldsymbol{A} + \boldsymbol{A}^* \odot \boldsymbol{A}_{\text{der}}$, here $\boldsymbol{A}_{\text{der}} = \left[\dfrac{\partial \boldsymbol{a}(\omega_1)}{\partial \omega_1}, \dfrac{\partial \boldsymbol{a}(\omega_2)}{\partial \omega_2}, \cdots, \dfrac{\partial \boldsymbol{a}(\omega_D)}{\partial \omega_D}\right]$. And CRB is obtained as

$$\text{CRB} = \frac{1}{L} (\boldsymbol{M}_f^H (\boldsymbol{I} - \boldsymbol{M}_s (\boldsymbol{M}_S^H \boldsymbol{M}_S)^{-1} \boldsymbol{M}_S^H) \boldsymbol{M}_f)^{-1} \qquad (17)$$

3.2   Complexity analysis

According to Ref.[28], for the traditional coprime sampling scheme, the complexity of estimating the covariance matrix is $O((M+N-1)^2 L)$, the complexity of making eigenvalue decomposition of it is $O(M+N-1)^3$, the complexity of spectral peak search is $O((M+N-1)DP)$, here P is the search accuracy. The total complexity is $O((M+N-1)^2 L + (M+N-1)^3 + (M+N-1)DP)$.

For the proposed segmented coprime sampling scheme in this paper, the MUSIC algorithm is replaced by the root-MUSIC, where the complexity of finding the root is $O(2(M+N-2)^3)$ and the total complexity is $O((M+N-1)^2 L + (M+N-1)^3 + 2(M+N-2)^3)$. The complexity comparison of the two algorithms is shown in Fig.3.
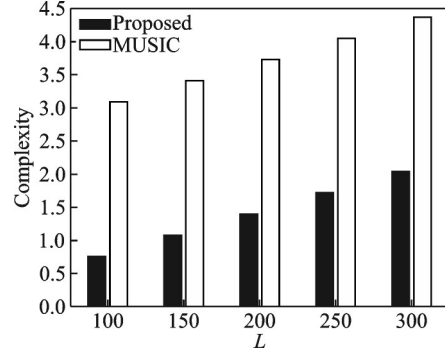

Fig.3   Complexity comparison

3.3   Advantages of the proposed scheme

Advantages of the proposed scheme are summarized as follows.

(1) The proposed scheme uses a sparse sampling method, which has a lower sampling rate than traditional uniform sampling.

(2) The proposed scheme uses root-MUSIC for analysis, which has lower computational complexity than the MUSIC algorithm.

(3) The proposed scheme is applicable to harmonic and interharmonic signals in power systems and is easy to implement in practice, enabling high precision frequency estimation.

4   Simulation Results

Assume that the received harmonic-containing signal is

$$x(t) = 0.2\cos(2\pi \times 25.2t) + \cos(2\pi \times 49.8t) + 0.5\cos(2\pi \times 151.5t) + e(t) \qquad (18)$$

This signal contains three frequency components: 50 Hz industrial frequency, 25 and 150 Hz interharmonics, and $e(t)$ is Gaussian white noise. According to Ref.[29], the signal frequency will fluctuate by 1%—2% on the power transmission line, and a certain error should be reasonably set.

The proposed scheme is evaluated using the root mean square error (RMSE) of the signal frequency estimation in the simulation. RMSE is shown as

$$\text{RMSE}_{\text{Fre}} = \frac{1}{D} \sum_{d=1}^{D} \sqrt{\frac{1}{K} \sum_{k=1}^{K} (\hat{\omega}_{d,k} - \omega_d)^2} \qquad (19)$$

where $\hat{\omega}_{d,k}$ is the estimated value of ω_d in the kth

Monte Carlo simulation, K the total number of simulations, and we take $K=200$ in the following simulation.

4. 1 Frequency estimation results

According to Ref. [29], it is reasonable to assume that the main components in the harmonic-containing signal include the fundamental wave, the third harmonic and the inter-harmonic less than the power frequency to determine $D=3$ in Eq.(8).

Fig.4 illustrates the estimation results of the frequency principal components under different conditions. In Fig.4, we set L to 300, and SNR is uniformly increased from 5 dB to 30 dB. In Fig.5, we set SNR to 20 dB, and L increases evenly from 100 to 1 000. It can be seen from the simulation results that the proposed method can effectively estimate the main frequency components in the signal.
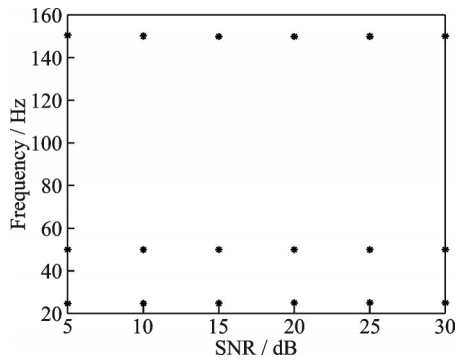

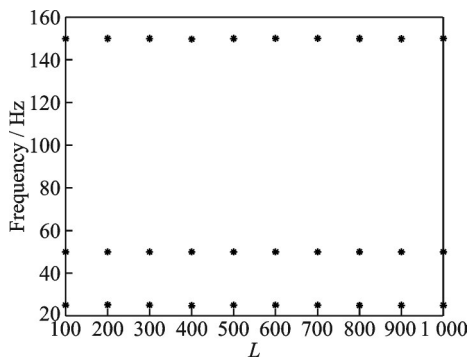Fig.4 Frequency estimation with different SNR

Fig.5 Frequency estimation with different L

4. 2 Performance of stability

In order to verify the stability of the proposed scheme, we set a set of signals with frequency fluctuations, and the frequencies to be measured, $f_1=$

25 Hz, $f_2=50$ Hz, $f_3=150$ Hz, all have $1\%—2\%$ fluctuations.

Fig.6 illustrates the line graph of RMSE with the number of experiments of the proposed scheme. We set $M=4$, $N=5$, $L=300$, SNR=20 dB, and the algorithm is simulated over 100 times. Despite low SNR, the scheme can still estimate frequency parameters effectively. Considering the fluctuation of the signal, under different number of experiments, RMSE tends to be stable, indicating that the scheme has good stability.
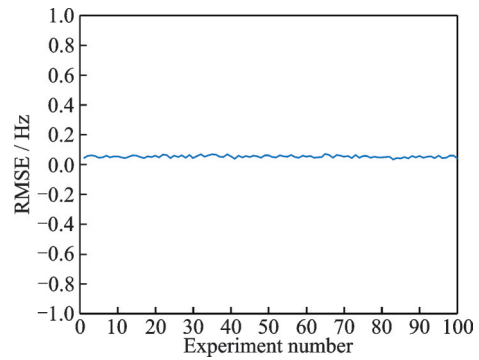

Fig.6 RMSE performance with different experiment numbers

4. 3 Performance of different sampling schemes

Fig.7 illustrates the RMSE performance of the proposed scheme, the uniform sampling method[10], the nested sampling method[30] and the coprime sampling method[21] at different SNR. In the simulation, we set $L=300$, and SNR increases uniformly from 5 dB to 30 dB. In order to allow a fair comparison, the number of samples per unit of uniform sampling is $M+N-1=8$.
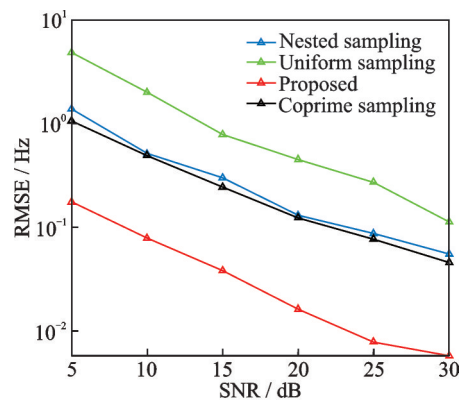

Fig.7 RMSE performance versus SNR with $L=300$

Fig.8 shows the RMSE performance of the proposed scheme, the uniform sampling method[10], the nested sampling method[30] and the coprime sampling method[21] with different L. Based on the simulation, SNR is set to 20 dB and L is increased uniformly from 100 to 1 000.
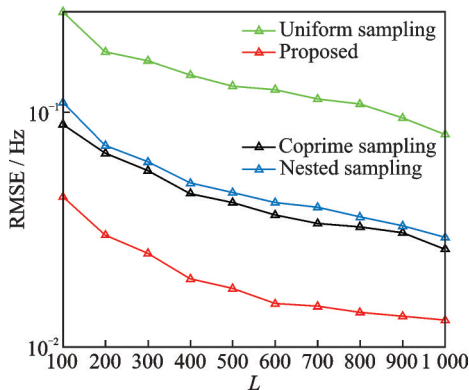

Fig.8   RMSE performance versus L with SNR=20 dB

As shown in Figs.7,8, RMSE of the proposed scheme is significantly lower than those of coprime sampling, uniform sampling, and nested sampling. Nested sampling can also reduce the sampling rate. However, nested sampling creates a continuous sampling structure that is ineffective in reducing the sampling rate.

5   Conclusions

We propose a scheme for estimating interharmonic frequencies by sparse sampling and spatial spectrum estimation algorithms. The sampling rate is reduced using sparse sampling, and then super-resolution estimation is performed using root-MUSIC. In addition, our proposed scheme does not impose an additional sampling burden on the sampler. The proposed scheme is applicable to harmonic and interharmonic signals in power systems, and the sparse sampling process reduces the sampling burden, while modern spectral estimation algorithms can obtain accurate frequency estimates.

References

［1］ CHIDURALA A, SAHA T K, MITHULANAN-THAN N. Harmonic impact of high penetration photo-voltaic system on unbalanced distribution networks-learning from an urban photovoltaic network[J]. IET Renewable Power Generation, 2015, 10(4): 485-494.

［2］ LANGELLA R, TESTA A, MEYER J, et al. Experimental-based evaluation of PV Inverter harmonic and interharmonic distortion due to different operating conditions[J]. IEEE Transactions on Instrumentation and Measurement, 2016, 65(10): 1-13.

［3］ ZAVODA F, RNNBERG S, BOLLEN M, et al. Power quality and EMC issues with future electricity networks[EB/OL]. (2018-03-01)[2022-07-20]. https://www.researchgate.net/publication/323796561.

［4］ HUANG Shan, ZHANG Haijian, SUN Hong, et al. Frequency estimation of multiple sinusoids with three sub-Nyquist channels[J]. Signal Processing, 2017, 139: 96-101.

［5］ SHI Jun, LIU Xiaoping, HE Lei, et al. Sampling and reconstruction in arbitrary measurement and approximation spaces associated with linear canonical transform[J]. IEEE Transactions on Signal Processing, 2016, 64(24): 6379-6391.

［6］ XU Y, LIU Y, LU M. Improved harmonic analysis based on quadruple-spectrum-line interpolation FFT with multiple cosine window[C]//Proceedings of 2017 First International Conference on Electronics Instrumentation & Information Systems (EIIS). [S.l.]: IEEE, 2017: 1-4.

［7］ RAVINDRAN V, BUSATTO T, RÖNNBERG S K, et al. Time-varying interharmonics in different types of grid-tied PV inverter systems[J]. IEEE Transactions on Power Delivery, 2020, 35(2): 483-496.

［8］ LI Chun. Unstable operation of photovoltaic inverter from field experiences[J]. IEEE Transactions on Power Delivery, 2018, 33(2): 1013-1015.

［9］ DAI J J, SHOKOOH F. Industrial and commercial power system harmonic studies[C]//Proceedings of 2021 IEEE/IAS 57th Industrial and Commercial Power Systems Technical Conference (I&CPS). [S.l.]: IEEE, 2021.

［10］ ZHAO Y, HU Y H, LIU J. Random Triggering-based sub-Nyquist sampling system for sparse multiband signal[J]. IEEE Transactions on Instrumentation and Measurement, 2017, 66(7): 1789-1797.

［11］ MISU T, MATSUO Y, SAKAIDA S, et al. Motion-adaptive sub-Nyquist sampling technique for multi-frame super-resolution[C]//Proceedings of 2012 Pic-

ture Coding Symposium.［S.l.］：IEEE, 2012: 321-324.

［12］ CHINTAKINDI S R, VARAPRASAD O, SARMA D. Improved Hanning window based interpolated FFT for power harmonic analysis［C］//Proceedings of IEEE Region 10 Conference. Macao, China：IEEE, 2016.

［13］ NOSHAHR J B, KALESAR B M. Harmonic spectrum estimation and analysis of the voltage at the PCC of the distribution network connected to solar plant based on parametric algorithm (Music)［C］//Proceedings of 2017 IEEE International Conference on Environment and Electrical Engineering.［S.l.］：IEEE, 2017：1-6.

［14］ SHI H, JIA B. SAR imaging method based on coprime sampling and nested sparse sampling［J］. Journal of Systems Engineering and Electronics, 2015. DOI：10.1109/JSEE.2015.00134.

［15］ ZHENG Wang, ZHANG Xiaofei, GONG Pan, et al. DOA estimation for coprime linear arrays：An ambiguity-free method involving full DOFs［J］. IEEE Communications Letters, 2018, 22(3)：562-565.

［16］ SI Q, ZHANG Y D, AMIN M G. Generalized coprime array configurations for direction-of-arrival estimation［J］. IEEE Transactions on Signal Processing, 2015, 63(6)：1377-1390.

［17］ DONG Xudong, ZHANG Xiaofei, ZHAO Jun, et al. DOA estimation for coprime array with mixed noise scenario via phased fractional low-order moment［J］. IEEE Wireless Communications Letters, 2021, 10(11)：2567-2571.

［18］ LI Bingying, DING Yuehua. Direction-of-arrival estimation of non-circular signals using nested array［C］//Proceedings of 2019 Computing, Communications and IoT Applications (ComComAp). Shenzhen, China：IEEE, 2019.

［19］ MOFFET A. Minimum-redundancy linear arrays［J］. IEEE Transactions on Antennas and Propagation, 1968, 16(2)：172-175.

［20］ LIU S, MA Y, TAO S. Segmented discrete polynomial-phase transform with coprime sampling［J］. The Journal of Engineering, 2019. DOI：10.1049/joe.2019.0312.

［21］ CHEN Luo, LIN Xinping, ZHU Beizuo, et al. Generalized parallel coprime array for two-dimensional DOA estimation：A perspective from maximizing degree of freedom［J］. China Communications, 2021(4)：14-26.

［22］ ZHOU Chengwei, ZHENG Hang, GU Yujie, et al. Research progress on coprime array signal processing：Direction-of arrival estimation and adaptive beamforming［J］. Journal of Radars, 2019, 8(5)：558-577. (in Chinese)

［23］ QIN Si, ZHANG Yimin, AMIN M G, et al. Generalized coprime sampling of Toeplitz matrices for spectrum estimation［J］. IEEE Transactions on Signal Processing, 2017, 65(1)：81-94.

［24］ LUO Q, ZHONG Q, WANG G, et al. An order-reduction method of interharmonic analysis model based on the principle of interharmonic interaction［J］. CPSS Transactions on Power Electronics and Applications, 2021,6(3)：209-217.

［25］ FU Zhe, CHARGÉ P, WANG Yide. Multi-rate coprime sampling for frequency estimation with increased degrees of freedom［J］. Signal Processing, 2020 (166)：107258.

［26］ VAIDYANATHAN P P, PAL P. Why does direct-MUSIC on sparse-arrays work?［C］//Proceedings of Conference on Signals.［S.l.］：IEEE, 2013.

［27］ LIU C L, VAIDYANATHAN P P. New Cramér-Rao bound expressions for coprime and other sparse arrays［C］//Proceedings of Sensor Array & Multichannel Signal Processing Workshop.［S.l.］：IEEE, 2016：1-5.

［28］ LIU C L, VAIDYANATHAN P P. Cramér-Rao bounds for coprime and other sparse arrays, which find more sources than sensors［J］. Digital Signal Processing, 2017, 61：43-61.

［29］ CHATTOPADHYAY S, MITRA M, SENGUPTA S, et al. Electric power quality［M］. Netherlands：Springer, 2011.

［30］ QIAO H, PAL P. Generalized nested sampling for compression and exact recovery of symmetric Toeplitz matrices［C］//Proceedings of 2014 IEEE Global Conference on Signal and Information Processing (GlobalSIP). Atlanta, GA, USA：IEEE, 2014.

Authors   Mr. **YUE Heng** received the B. E. degree in 2020, where he is pursuing the M.S.degree in communication and information systems at Nanjing University of Aeronautics and Astronautics, Nanjing, China. His current re-

search focuses on array signal processing.

Prof. **ZHANG Xiaofei** received the Ph.D. degree in communication and information systems from Nanjing University of Aeronautics and Astronautics, Nanjing, China, in 2005. Currently he is a professor at College of Electronic and Information Engineering, Nanjing University of Aeronautics and Astronautics. His research interests include array signal processing and communication signal processing.

Author contributions　Mr. **YUE Heng** designed the study, complied the models, simulated the algorithms, wrote the manuscript and participated the algorithm simulation work. Prof. **ZHANG Xiaofei** contributed to the data analysis and the background of this study. Both authors commented on the manuscript draft and approved the submission.

（Production Editor：ZHANG Huangqun）

基于分段互质采样的谐波和间谐波频率估计方法

岳　衡 [1,2]，张小飞 [1,2]

（1.南京航空航天大学天地一体频谱认知智能实验室，南京 211106，中国；

2.南京航空航天大学电子信息工程学院，南京 211106，中国）

摘要：电力系统中电力电子产生的谐波数量不断增加，谐波问题是一个重要的问题。本文提出了一种改进的互质采样（Coprime sampling，CS）方案，用于谐波和间谐波频率估计。所提方案使用稀疏采样来降低采样率，并将其与现代频谱估计算法相结合。特别是，使用分段互质采样（Segmented coprime sampling，SCS）方法，然后使用求根多重信号分类（Root-multiple signal classification，root-MUSIC）算法代替常用的 MUSIC 算法可以减少计算工作量并获得准确的频率估计。仿真结果表明，该方法在估计精度上优于传统的均匀采样（Uniform sampling，US）方法。

关键词：互质采样；间谐波；root-MUSIC 算法；频率估计